

Identification of inherent noise components of semiconductor devices on an example of optocouplers

B. STAWARZ-GRACZYK*, A. SZEWCZYK, and A. KONCZAKOWSKA

Faculty of Electronics, Telecommunications and Informatics, Gdańsk University of Technology,
11/12 Narutowicza Str., 80-952 Gdańsk, Poland

In the paper, a method of estimation of parameters of Gaussian and non-Gaussian components in the noise signal of semiconductor devices in a frequency domain is proposed. The method is based on composing estimators of two spectra, corresponding to $1/f^\alpha$ noise (Gaussian component) and two-level RTS noise (non-Gaussian component). The proposed method can be applied for precise evaluation of the corner RTS frequency f_{RTS} in the noise spectrum.

Keywords: $1/f^\alpha$ noise, RTS noise, Gaussian component, non-Gaussian component, optocouplers, spectra estimating.

1. Introduction

The properties of low-frequency noise of semiconductor devices can be defined on the basis of an identification of two components:

- a component whose instantaneous values of low-frequency noise have Gaussian distribution, shortly named “Gaussian” component and,
- a component whose instantaneous values of low-frequency noise have non-Gaussian distribution, shortly named “non-Gaussian” component [1–3].

The non-Gaussian component can be absent in low-frequency noise, but if occurs, its identification can give additional information about the quality of the device under test [4,5].

In order to identify these components, the low-frequency noise analysis can be carried out in the time domain or in the frequency domain. Usually, in the time domain, the noise signal is recorded and a histogram of its instantaneous values is estimated, while in the frequency domain the estimation refers to a spectrum and often to a product of spectrum and frequency. Sometimes, the methods mentioned above are not enough precise to identify the non-Gaussian component.

The aim of the paper is to propose a method of identification of Gaussian and non-Gaussian component parameters of a noise signal in the frequency domain. Typically, a Gaussian component of the low-frequency noise signal of semiconductor devices is caused by thermal, shot, and $1/f^\alpha$ noise and the non-Gaussian component is caused by a single generation-recombination centre (two-level RTS noise) or by generation-recombination centres (multi-level RTS noise). It is obvious that in the low-frequency range in a Gaussian component, the dominant noise is $1/f^\alpha$ noise. In our discussion it was assumed that the non-Gaussian com-

ponent is caused by two-level RTS noise. That is why the presented method is based on composing the estimators of two spectra corresponding to $1/f^\alpha$ noise (Gaussian component) and RTS noise (non-Gaussian component).

In a frequency domain, the Gaussian component of a noise signal can be described by two parameters, the noise coefficient K_f and the $1/f^\alpha$ spectrum slope α . The spectrum is estimated by the following relation

$$S_{1/f} = \frac{K_f}{f^\alpha}. \quad (1)$$

In the time domain, the RTS noise signal can be described by three parameters the amplitude A , the mean time the impulse remains in the up state t_{up} , and the mean time the impulse remains in the down state t_{down} . The durations of t_{up} and t_{down} are independent random variables with a Poisson distribution. The RTS noise characteristic frequency (corner frequency) can be expressed by Eq. (2)

$$f_{RTS} = \frac{1}{2\pi} \left(\frac{1}{t_{up}} + \frac{1}{t_{down}} \right). \quad (2)$$

The f_{RTS} is the parameter of RTS noise that can be estimated from the spectrum in the frequency domain as the frequency at which the plateau comes into $1/f^2$. In the frequency domain, the non-Gaussian component of noise (two-level RTS noise) can be described by two parameters, the level (intensity) of the plateau A and by the corner frequency f_{RTS} . The spectrum of a pure two-level RTS signal is Lorentzian and it is given by the following relation

$$S_{RTS} = \frac{A}{1 + \left(2\pi \frac{f}{f_{RTS}} \right)^2}. \quad (3)$$

* e-mail: bstawarz@eti.pg.gda.pl

The proposed method consists of fitting one spectrum or two spectra to a “real” spectrum, which was estimated from the noise signal of the tested semiconductor device. It should be emphasized that in practice if only one component is present, it is the Gaussian component.

In case of one component (Gaussian), one should estimate the following parameters of the noise spectrum K_f and α . In case of two components (Gaussian and non-Gaussian), one should estimate the following parameters of the noise spectrum K_f , α , A , and f_{RTS} .

The presented method of identification of low-frequency noise components can be applied for different kinds of semiconductor devices. In the paper, it is applied to CNY 17 optocouplers as an example.

The CNY 17 optocoupler is a gallium arsenide infrared light emitting diode optically coupled with a silicon NPN phototransistor. The low-frequency noise of optocouplers was measured in the frequency range of 10–1500 Hz. Detailed results of noise measurements for those devices are presented mainly in Refs. 1, 5, and 6.

2. Measurement results

The results presented in Refs. 1 and 7 show that there are either one (Gaussian) or two (Gaussian and non-Gaussian) components in optocoupler inherent noise. Furthermore, for most of

devices, the identification of components in the time domain as well as in the frequency domain is obvious. However, there are some devices for which the identification of presence of a non-Gaussian component in the noise signal is not straightforward. As an example, the low-frequency noise data of an optocoupler showing only a Gaussian component (device A) or both components (device B) and with not obvious presence of non-Gaussian component (device C) are selected and presented below.

2.1. Time domain

The results of low-frequency noise measurements of device A and device B (observed noise and histogram) are presented in Figs. 1 and 2, respectively. The presented results are for the diode current $I_D = 5$ mA and the collector-emitter voltage $U_{CE} = 5$ V.

In the noise signal presented in Fig. 1(a) and also in the histogram shown in Fig. 1b, the Gaussian character of instantaneous values distribution is clearly seen, whereas in the noise signal shown in Fig. 2(a) one can see the RTS noise and the histogram in Fig. 2(b) shows a bimodal distribution (two-level RTS noise).

Figure 3 presents the noise signal and the histogram of device C. In its low-frequency noise signal, the non-Gaussian component cannot be clearly identified and the histogram does not have a bimodal distribution.

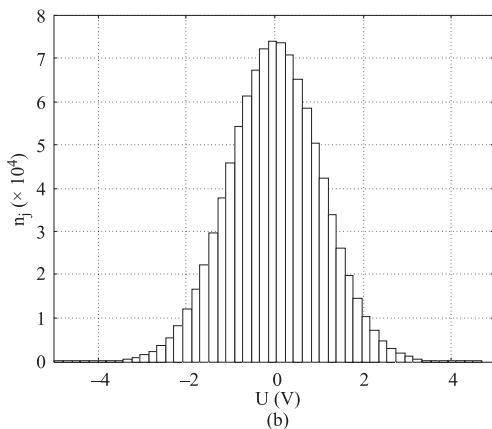
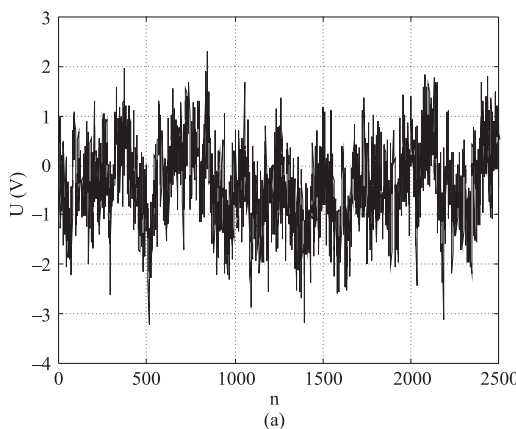


Fig. 1. Observed noise (a) and histogram of device A (b).

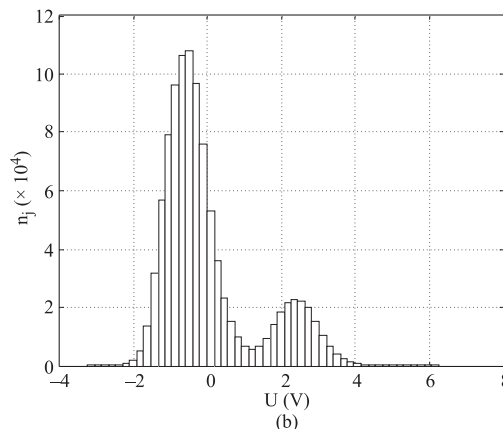
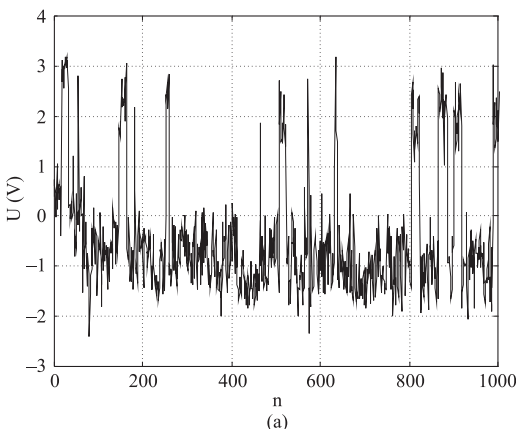


Fig. 2. Observed noise (a) and histogram of device B (b).

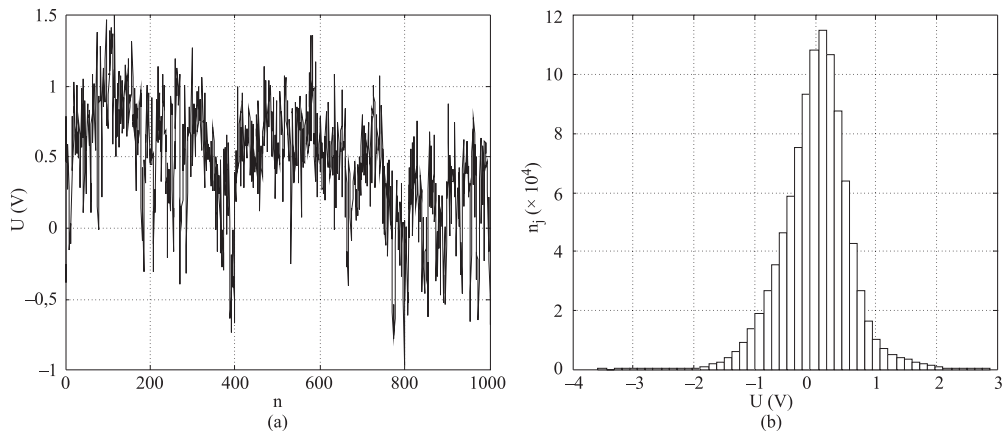


Fig. 3. Observed noise (a) and histogram of device C (b).

To test if the distribution of low-frequency noise is normal, a normality test can be applied. For the presented data, the $n\Omega^2$ test was used [8,9]. During the test, the assumption was made that the noise instantaneous values have a normal distribution and this hypothesis is not rejected with the confidence level equal to $\alpha = 0.05$ when

$$\omega_n^2 < (\Omega_{1-\alpha})^2. \quad (4)$$

The value of $(\Omega_{1-\alpha})^2$ is read from the table and in this case is equal to 0.46136. The ω_n^2 parameter is equal to

$$\omega_n^2 = \frac{1}{12 \cdot n} + \sum_{i=1}^n [F(t_{(i)}) - F^*(t_{(i)})]^2, \quad (5)$$

where $i = 1, 2, \dots, N$, n is the realization number taken into account, $F(t_{(i)})$ is the value of the tested theoretical standard normal cumulative distribution, and $F^*(t_{(i)}) = i/(n+1)$ is the value of the standard normal cumulative distribution.

The results of the $n\Omega^2$ test for devices A, B, and C are compared in Table 1 where “+” means that the hypothesis is not rejected and “-” means that the hypothesis is rejected.

 Table 1. Results of the $n\Omega^2$ test for optocouplers.

Device	w_n^2	Test result
A	0.05377	+
B	23.59819	-
C	1.94275	-

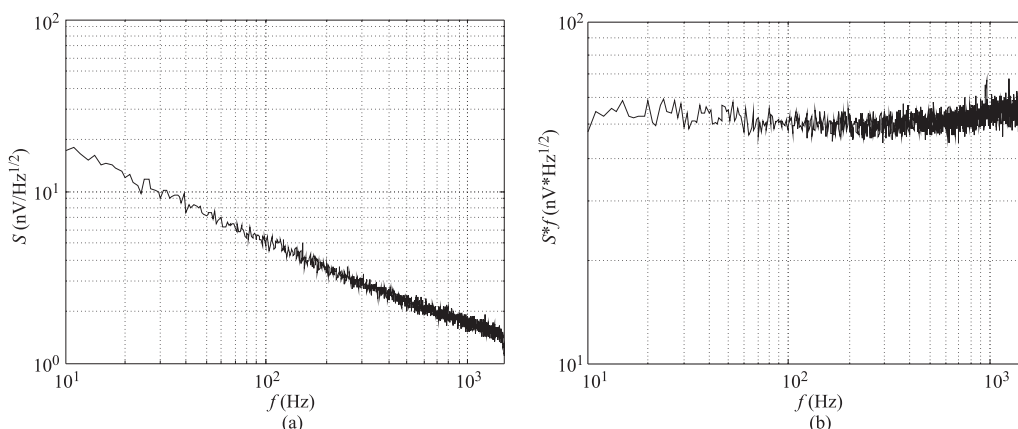
Taking into account the data in Figs. 1–3 and $n\Omega^2$ test results it can be pointed out that:

- only a Gaussian component is observed in the noise of device A,
- non-Gaussian component occurrence is clearly visible in the noise of device B,
- $n\Omega^2$ test hypothesis was rejected for devices B and C,
- w_n^2 value for device B is much greater than for device C.

2.2. Frequency domain

For the data from Figs. 1 and 3, the power spectral density (PSD) and the product of PSD and frequency were calculated. The results are shown in Figs. 4, 5, and 6, respectively.

The Gaussian component is observed in the PSD of device A whereas the non-Gaussian component can be precisely identified only in device B as the plateau in Fig. 5(a)


 Fig. 4. PSD (a) and $f S(f)$ product estimated for device A (b).

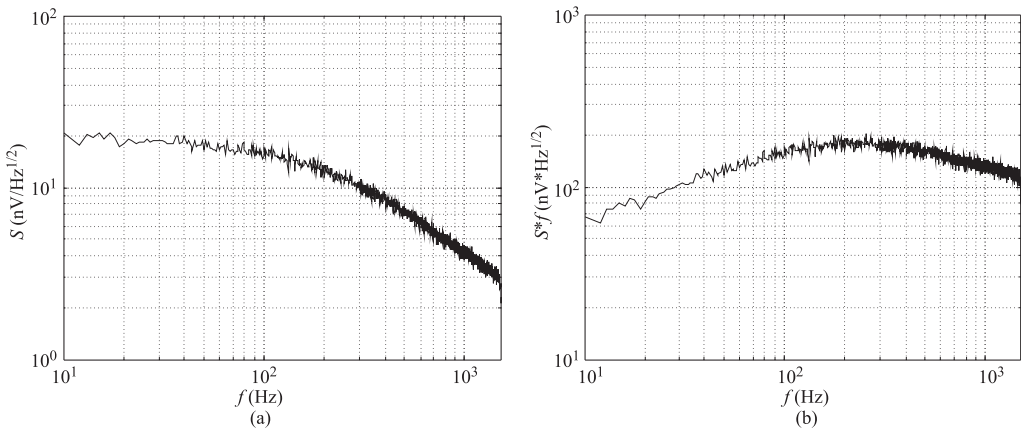


Fig. 5. PSD (a) and $fS(f)$ product estimated for device B (b).

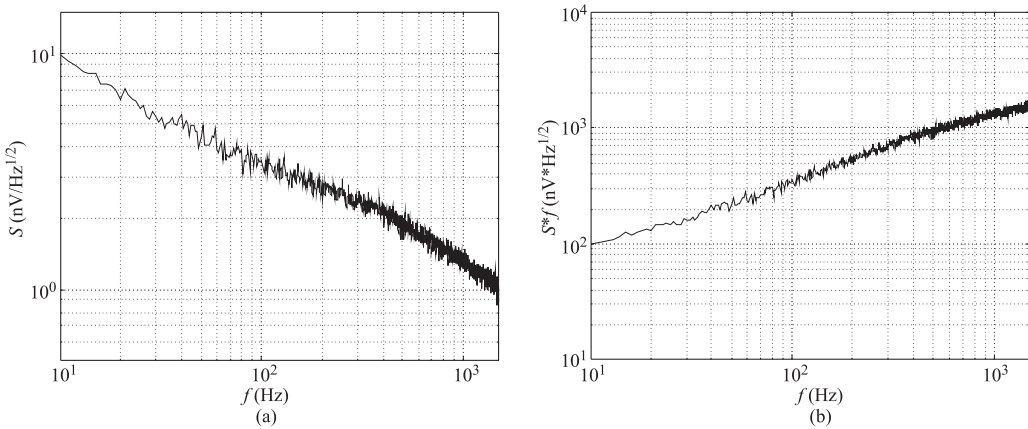


Fig. 6. PSD (a) and $fS(f)$ product estimated for device C (b).

and as a local maximum in Fig. 5(b) at a frequency of about 200 Hz.

In PSD of device C, only the Gaussian component is easily identified. The occurrence of a non-Gaussian component was only found due to the $n\Omega^2$ test (see results in Table 1). This example shows that not all components can be identified in PSDs as well as the values of their parameters, especially f_{RTS} . For that, in our opinion, there was a need to propose a method of precise component identification in the frequency domain presented in the next chapters.

3. Noise model

The tool proposed in the paper allows us to estimate the components of a noise signal particularly to identify the parameters of the Gaussian ($1/f^\alpha$ noise) and non-Gaussian component (RTS noise). For this purpose, the presented model consists of two modules. The first one is responsible for generating the proper $1/f^\alpha$ noise signal, the other one generates RTS noise. The modules are presented below.

3.1. $1/f^\alpha$ noise signal generator

The $1/f^\alpha$ noise signal generator was designed in the Micro-Cap program as an noise macromodel of an optocoupler with the possibility of changing the value of the exponent α ,

which was only available due to a MOSFET transistor (MTP15N06L) [10,]. The circuit with an enhanced optocoupler's macromodel is presented in Fig. 7.

The optocoupler's macromodel with the possibility of changing the value of the exponent α is contained within the dotted frame. The $1/f^\alpha$ noise signal with specific parameters (K_f and α) simulated in the enhanced optocoupler's macromodel is stored in a text file.

3.2. RTS noise signal generator

The RTS noise signal is generated in a LabView virtual instrument (vi). The program generates a two-level RTS noise signal with random length of impulses and random distance between them. The input data are as follows:

- number of samples N ,
- sampling frequency f_s ,
- signal amplitude A ,
- RTS corner frequency f_{RTS} ,
- mean signal duty factor c .

The duration in seconds of the generated signal is equal to N/f_s , the mean time the impulse remains in up and down state are respectively equal to

$$t_{up} = \frac{1}{2 \cdot \pi \cdot f_{RTS} \cdot (1 - c)}, \quad (6)$$

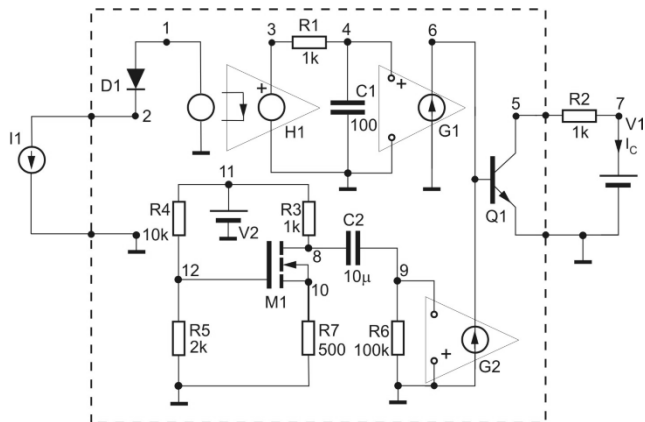


Fig. 7. A circuit with enhanced macromodel of an optocoupler with $1/f^\alpha$ noise source.

$$t_{down} = t_{up} \frac{1-c}{c}. \quad (7)$$

Afterwards the program calculates t_{up} and t_{down} [according to Eqs. (6) and (7)], the random value r from the range $\langle 0,1 \rangle$ is generated by the built-in random number generator with uniform distribution. The value r is utilised to calculate the random variable corresponding with the length of impulse duration in the up state [Eq. (8)] or the length of impulse duration in the down state [Eq. (9)]

$$t_1 = -t_{up} \cdot \ln(r), \quad (8)$$

$$t_2 = -t_{down} \cdot \ln(r). \quad (9)$$

Finally, the vi adds to the generated signal the t_1 samples of the value A or t_2 samples of the value 0 if the signal is in up or down state, respectively. The vi finishes its work when the generated signal length exceeds N samples. For simplification of the calculations presented below, it was assumed that the RTS noise signal designed duty factor c is equal to 0.5, it means that the t_{up} is the same as the t_{down} .

4. Description of spectra estimating

In order to compose a spectrum which would be identical with the measured “real” spectrum, the macro in MS Excel was elaborated. As the input data, macro collects the measured spectrum and the files with PSDs Gaussian component $1/f^\alpha$ noise signal and non-Gaussian component – RTS noise signal. Afterwards, the proper graphs are elaborated. In case that the estimated spectrum is not identical with the measured one, the macro enables to correct and to set the appropriate level and slope of $1/f^\alpha$ and the right level of the RTS noise signal.

In Fig. 8, an exemplary simulation for device A (the one without non-Gaussian component) is presented.

As one can see above, the generated Gaussian component perfectly fits the measured spectrum. The estimated parameters K_f and α are collected in Table 2.

The component identification for device B (the one with visible RTS noise signal) is presented in Fig. 9.

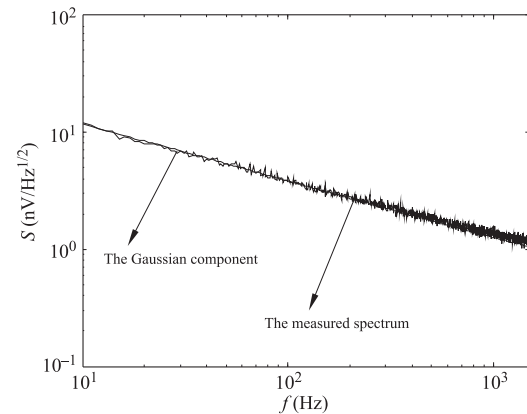


Fig. 8. Measured spectrum and a Gaussian component of a spectrum for device A.

After the parameters of Gaussian component ($1/f^\alpha$ noise signal) and non-Gaussian component (RTS noise signal) for device B were selected properly, the composed spectrum was identical with the measured one. The estimated parameters K_f , α , A , and f_{RTS} are collected in Table 2.

Table 2. Identification of component parameters for devices A, B, and C.

Device	Gaussian component ($1/f^\alpha$ noise)		Non-Gaussian component (RTS noise)			
	K_f (V^2)	α	A (V^2)	f_{RTS} (Hz)	t_{up} (ms)	t_{down} (ms)
A	14.36×10^{-16}	1.0	–	–	–	–
B	6.15×10^{-16}	1.1	4.53×10^{-14}	250	1.27	1.27
C	43.03×10^{-16}	1.4	19.18×10^{-16}	130	2.45	2.45

The measured spectra presented in Figs. 8 and 9 are quite easy to be concerned as free of RTS noise (device A) and consisting RTS noise (device B), respectively. The measured spectrum presented in Fig. 6 (device C) may seem to be free of RTS noise. The elaborated method of component identification shows that a non-Gaussian component

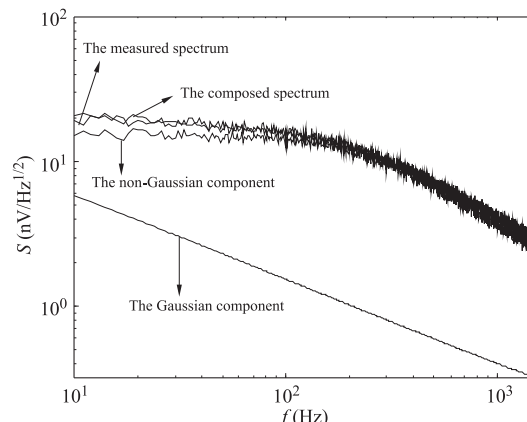


Fig. 9. Measured spectrum, components of a spectrum and a composed spectrum for device B.

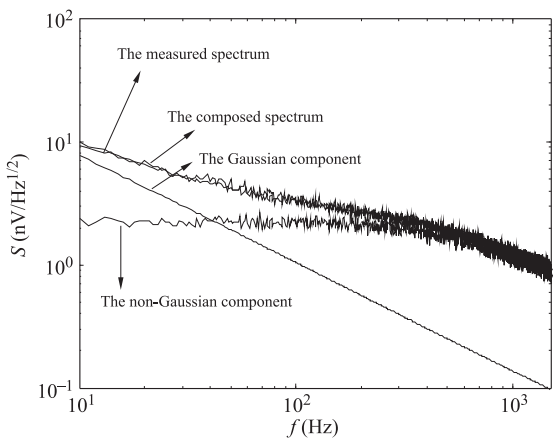


Fig. 10. Measured spectrum, components of a spectrum and a composed spectrum for device C.

occurs in the noise signal (Fig. 10). The estimated parameters K_f , α , A , and f_{RTS} are collected in Table 2.

As mentioned before, the presented method allows us to identify the parameters of noise components.

In Table 2, the values of the time t_{up} and t_{down} are also presented but they are only for theoretical modelling. Figure 10 shows that the level of RTS noise is lower than the level of measured spectrum, definitely the $1/f^\alpha$ noise dominates in device C. Moreover, the levels of RTS and $1/f^\alpha$ noise are quite similar. The opposite situation is in device B (Fig. 9) where the level of RTS noise is practically equal to the level of the measured spectrum and the RTS noise clearly dominates in the whole frequency range.

5. Conclusions

In the paper, the course of identification of components of inherent noise of semiconductor devices was described. The results of spectra composing presented on examples of devices A, B, and C allow us to assume that the method of component identification works properly and very precisely. Even non-Gaussian components with a very low amplitude of RTS noise, weakly visible in a spectrum or a histogram can be identified by the method. An example of such

identification was shown for device C. The method allows us to estimate the components intensity.

The advantage of the method is also the possibility of identification of all component parameters such as K_f , α , A , f_{RTS} , t_{up} and t_{down} .

References

1. A. Konczakowska, J. Cichosz, A. Szewczyk, and B. Stawarz, "Identification of optocoupler devices with RTS noise", *Fluctuation and Noise Letters* **6**, L395–L404 (2006).
2. A. Konczakowska, J. Cichosz, and A. Szewczyk, "A new method for identification of RTS noise", *Bull. Pol. Ac.: Tech.* **54**, 457–460 (2006).
3. A. Konczakowska, J. Cichosz, and A. Szewczyk, "A new method for RTS noise of semiconductor devices identification", *IEEE T. Instrum. Meas.* **57**, 1199–1206 (2008).
4. L.K.J. Vandamme and M. Macucci, "1/f and RTS noise in submicron devices: Faster is noisier", *AIP Conf. Proc.* **800**, 436–443 (2005).
5. A. Konczakowska, "Szumy z zakresu małych częstotliwości. Metody pomiaru, zastosowanie do oceny jakości przyrządów półprzewodnikowych", *Akademicka Oficyna Wydawnicza EXIT*, Warszawa (2006). (in Polish)
6. A. Konczakowska, J. Cichosz, and B. Stawarz, "RTS noise in optoelectronic coupled devices", *Proc. 18th Inter. Conf. Noise and Fluctuations ICNF'2005*, Salamanca, 669–672 (2005).
7. A. Konczakowska, J. Cichosz, A. Szewczyk, and B. Stawarz, "Analysis of noise properties of the optocoupler device", *Opto-Electron. Rev.* **15**, 149–153 (2007).
8. A. Balicki and W. Makać, "Metody wnioskowania statystycznego", *Wydawnictwo Uniwersytetu Gdańskiego*, 2002. (in Polish)
9. S. Lesiński, "Wzory i tablice do obliczeń niezawodności urządzeń elektrycznych", *Wydawnictwo Politechniki Łódzkiej*, 1995. (in Polish)
10. B. Stawarz-Graczyk, J. Cichosz, and A. Konczakowska, "Szumowy model transoptora z uwzględnieniem źródeł szumów typu $1/f^\alpha$ ", *Materiały VI Krajowej Konferencji Elektroniki, KKE' 2007, Darłówko Wschodnie*, tom 2, 461–466 (2007). (in Polish)
11. B. Stawarz-Graczyk, J. Cichosz, and A. Konczakowska, "The noise macromodel of an optocoupler including noise source", *Bull. Pol. Ac.: Tech.* **56**, 59–63 (2008).